Mutations in *Hydin* impair ciliary motility in mice

Karl-Ferdinand Lechtreck,[1] Philippe Delmotte,[2] Michael L. Robinson,[3] Michael J. Sanderson,[2] and George B. Witman[1]

[1]Department of Cell Biology and [2]Department of Physiology, University of Massachusetts Medical School, Worcester, MA 01655
[3]Zoology Department, Miami University, Oxford, OH 45056

Chlamydomonas reinhardtii hydin is a central pair protein required for flagellar motility, and mice with *Hydin* defects develop lethal hydrocephalus. To determine if defects in *Hydin* cause hydrocephalus through a mechanism involving cilia, we compared the morphology, ultrastructure, and activity of cilia in wild-type and *hydin* mutant mice strains. The length and density of cilia in the brains of mutant animals is normal. The ciliary axoneme is normal with respect to the 9 + 2 microtubules, dynein arms, and radial spokes but one of the two central microtubules lacks a specific projection. The *hydin* mutant cilia are unable to bend normally, ciliary beat frequency is reduced, and the cilia tend to stall. As a result, these cilia are incapable of generating fluid flow. Similar defects are observed for cilia in trachea. We conclude that hydrocephalus in *hydin* mutants is caused by a central pair defect impairing ciliary motility and fluid transport in the brain.

Introduction

Most motile cilia and flagella have a 9 + 2 axoneme containing nine peripheral doublet microtubules and two central microtubules. The axoneme also contains dynein arms and radial spokes that, together with the central pair (CP) of microtubules, generate and regulate motility. In mammals, motile 9 + 2 flagella are present on spermatozoa and motile 9 + 2 cilia are present on epithelial cells lining the airway, oviduct, and ventricles of the brain. In mice, CP defects result in severe impairment of sperm motility (Sapiro et al., 2002); in humans, 9 + 0 airway cilia from primary ciliary dyskinesia (PCD) patients lacking the CP perform an unusual whirling type of movement (Chilvers et al., 2003). This suggests that the CP is necessary for the stereotypical waveform of the mammalian cilium. This is consistent with evidence from lower organisms that the CP interacts with the radial spokes to control the activity of the dynein arms through a regulatory pathway that is important for normal ciliary movement (Smith, 2002).

The CP apparatus consists of two microtubules displaying several projections and connectors (Smith and Lefebvre, 1997). In *Chlamydomonas reinhardtii*, mutants with a defective central apparatus swim slowly, have abnormal flagellar waveforms, or are paralyzed. The structural defects range from lack of individual projections to loss of the entire CP. Several components of the central apparatus of *C. reinhardtii* have been identified (Witman et al., 1978; Dutcher et al., 1984; for review see Smith and Yang, 2004), including the ~540-kD protein hydin (Lechtreck and Witman, 2007). Hydin was found in the flagellar proteomes of the protists *C. reinhardtii* (Pazour et al., 2005) and *Trypanosoma brucei* (Broadhead et al., 2006), and comparative genomics indicates that the encoding gene is present broadly in organisms with the ability to assemble motile 9 + 2 cilia (Li et al., 2004). The knockdown of hydin in *C. reinhardtii* resulted in the loss of a specific projection from the central apparatus (Lechtreck and Witman, 2007). Hydin-deficient flagella exhibited paralysis with arrest at the end of the effective or recovery stroke; those displaying residual motility often stopped for extended periods of time at these same positions, where the direction of the beat is reversed. Based on these observations, it was postulated that hydin is a component of a CP projection involved in switching the activity of dynein arms between opposite halves of the axoneme during the transitions between effective and recovery strokes. Knockdown of hydin in *T. brucei* similarly resulted in CP defects and the loss of flagellar motility (Dawe et al., 2007).

Mice defective in *Hydin* develop hydrocephalus with early perinatal onset, and most animals die by 3 wk after birth (Raimondi et al., 1976; Davy and Robinson, 2003). Two mutant alleles of *Hydin* have been characterized. *hy3*, a spontaneous mutation first described by Gruneberg (1943), carries a single base pair deletion that causes a premature stop that would result in the loss of 89% of the full-length gene product (Davy and Robinson, 2003). The insertional mutation *OVE459* is characterized by genomic rearrangement around the insertion site within the *Hydin* gene (Robinson et al., 2002; Davy and Robinson, 2003).

Correspondence to K.-F. Lechtreck: Karl.Lechtreck@umassmed.edu; or G.B. Witman: George.Witman@umassmed.edu

Abbreviations used in this paper: CBF, ciliary beat frequency; CP, central pair; P, postnatal day; PCD, primary ciliary dyskinesia; SEM, scanning EM; Spag6, sperm-associated antigen 6; TEM, transmission EM.

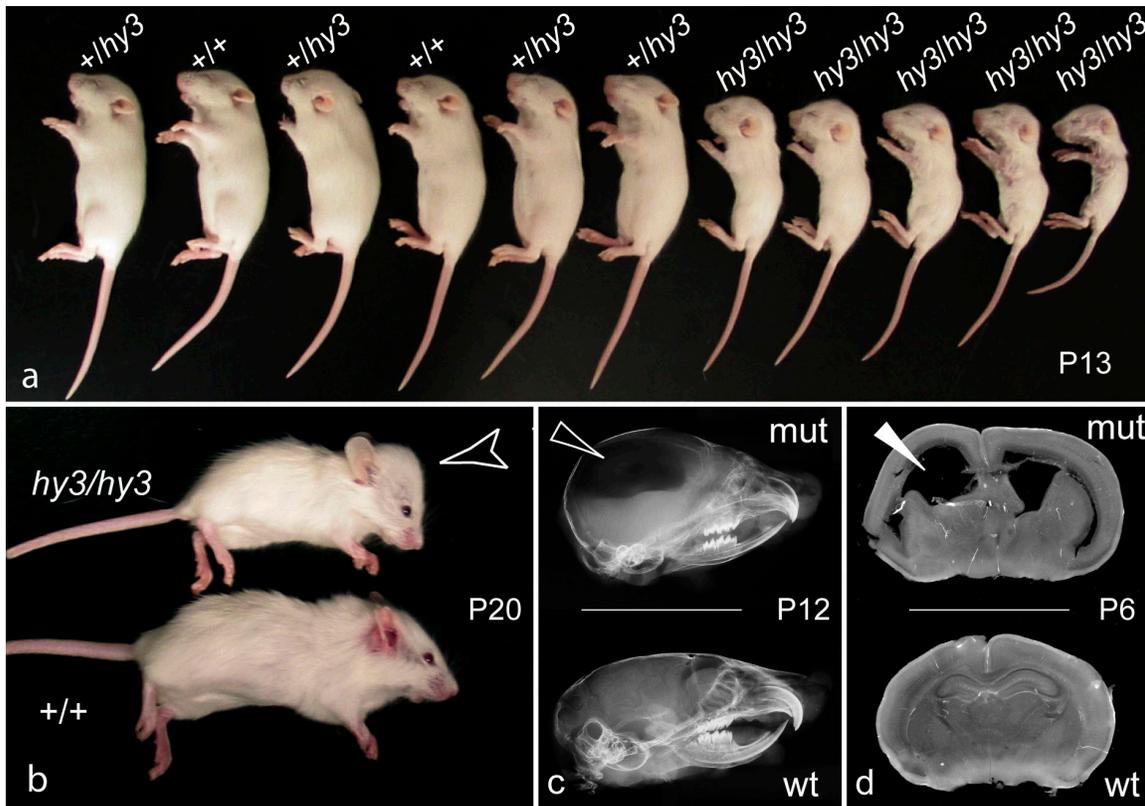The online version of this paper contains supplemental material.

Figure 1. **Gross analysis of *hydin* mutant mice.** (a) 11 pups from one litter on P13. The genotype is indicated. Note the growth retardation of the *hy3/hy3* mice. (b) *hy3/hy3* mutants develop hydrocephalus, which causes a dome-shaped skull (arrowhead). +/+, wild-type littermate. (c) X-ray images of hemisections through the skulls of a hydrocephalic animal (mut, *OVE459*) and a wild-type (wt) littermate. Arrowhead indicates the large radio-translucent cavity in the brain. (d) Coronal brain sections from wild-type and mutant (*OVE459*) littermates. Arrowhead indicates dilated lateral ventricle.

The two alleles do not complement each other and Northern analysis failed to detect *hydin* transcripts in these mutants. In the wild type, *Hydin* is expressed in developing spermatocytes and in epithelia lining the brain ventricles, the oviduct, and the airways (Davy and Robinson, 2003). This expression pattern correlates with the presence of motile cilia. This, together with the results from *C. reinhardtii* and *T. brucei*, suggests that hydrocephalus in *hydin* mutants is caused by defects in the ependymal cilia of the brain. Indeed, hydrocephalus has been reported for mice, rats, dogs, and humans with PCD, a disorder impairing ciliary motility (Torikata et al., 1991; Daniel et al., 1995; Afzelius, 1999). In humans, the *HYDIN* gene is located within a 1.2-Mb fragment to which a hydrocephalus-associated translocation has been mapped (Callen et al., 1990; Doggett et al., 2006), which suggests that defects in *HYDIN* also may cause hydrocephalus in humans.

Here, we analyzed the structure and movement of motile cilia from the brain and airways of *hydin* mutant mice and observed the specific loss of a projection from one of the central microtubules. Mutant cilia were unable to bend properly and frequently stalled, which is indicative of a defect in the regulation of dynein arm activity. As a consequence, cilia-generated flow was severely impaired. We conclude that hydrocephalus in *hydin* mouse mutants is caused by a CP defect and predict that humans with *HYDIN* mutations will have a higher than normal risk of developing hydrocephalus because of similar defects.

Results

To study the effect of Hydin deficiency on ciliary assembly and motility, two mouse strains carrying mutant alleles of *Hydin*, *hy3* and *OVE459*, were analyzed. Several mutations impairing ciliary motility or assembly are accompanied by a randomization of the body axis (Fliegauf et al., 2007). However, in *hy3/hy3* mice, situs abnormalities, as judged by the analysis of lung lobation as well as liver and stomach position in several dozen animals, were not observed. Affected animals could be identified at the earliest on postnatal day 4 (P4) by retarded growth and dome-shaped skulls (Fig. 1, a and b). In x-ray images of hemisections through the heads of mutants, a large radio-translucent cavity, caused by the accumulation of fluid in the brain, was visible (Fig. 1 c). The gross anatomy of brains from mutants revealed a smaller brain stem and cerebellum as well as smaller olfactory bulbs and, in strongly affected animals, severe hemorrhage below the skull (not depicted). Coronal sections through the brain demonstrated that the lateral and third ventricles of mutant animals were dilated (Fig. 1 d). Scanning EM (SEM) revealed that cilia were present on the ventricular epithelium of a 1-wk-old *hydin* mutant; the density and length of cilia were similar to that of its wild-type sibling (Fig. S1, a and b, available at http://www.jcb.org/cgi/content/full/jcb.200710162/DC1). Cilia also appeared normal in the trachea of wild-type and mutant animals (Fig. S1, c–f). In conclusion, Hydin deficiency does not interfere with ciliary
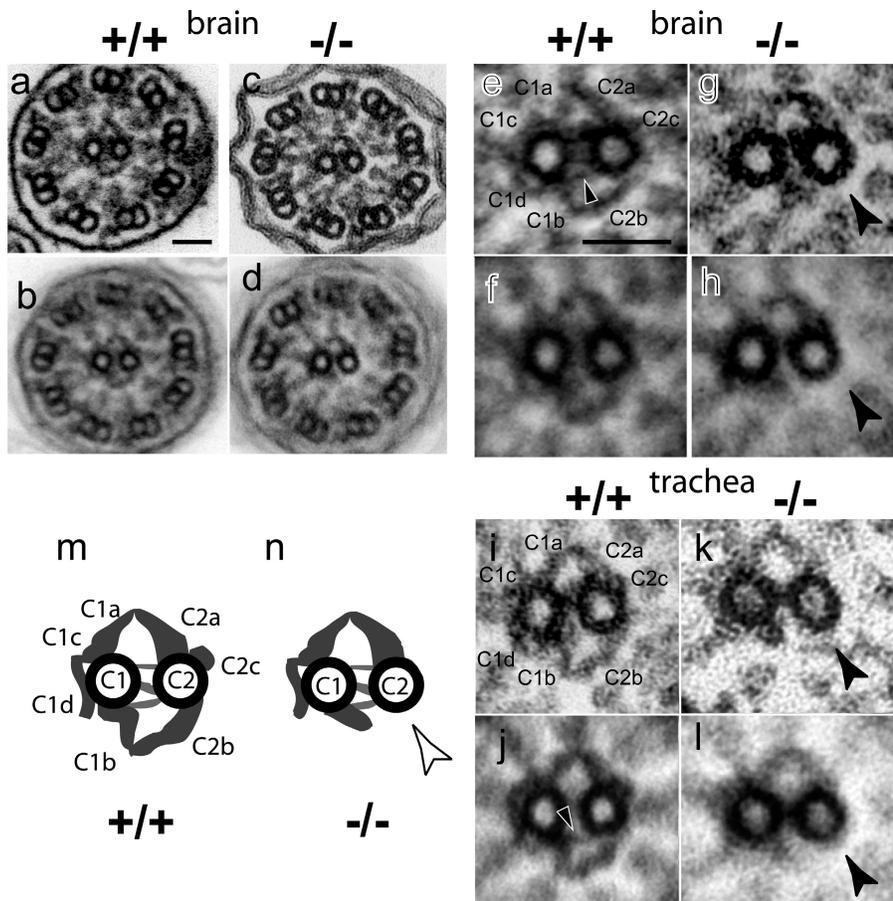
Figure 2. **Hydin deficiency causes a CP defect.** Ependymal cilia (a and c) and image averages (b and d) of ependymal cilia from wild-type (+/+, a and b) and *hy3/hy3* (−/−, c and d) animals. (e–h) Details of a–d, respectively, showing the CP of microtubules. (i–l) Details of the CP of wild-type (i) and mutant (k) tracheal cilia and image averages of wild-type (j) and mutant (l) tracheal cilia. Image averages are based on 5 (f), 13 (h), 10 (j), and 8 (l) images. (m and n) Diagram of the CP apparatus in wild-type (m) and mutant cilia (n). The CP projections are labeled in e, i, and m. The arrowhead in e and j indicates the diagonal link between the C1b projection and the C2 microtubule. The arrowhead in g, h, k, l, and n indicates the missing C2b projection in the CP of *hydin* mutants. Bars, 50 nm.

assembly in mice. In subsequent experiments, mutant animals between P5 and 8 exhibiting very little or no hydrocephalus and their wild-type littermates were used. Animals rarely survived beyond 3 wk, so sperm assembly and motility was not assessed.

Cilia of Hydin mutants lack a CP projection

Transmission EM (TEM) of ependymal cilia revealed the characteristic 9 + 2 structure of the axoneme and the presence of inner and outer dynein arms and radial spokes in both mutant and wild-type animals (Fig. 2, a–d). However, the pattern of projections attached to the two central microtubules was altered in the mutant and at least one of the projections was absent (Fig. 2, e–h). The CP is an asymmetrical structure because its two microtubules, termed C1 and C2, differ in the number and periodicity of the attached projections (Hopkins, 1970; Olson and Linck, 1977). The intrinsic structural asymmetry of the central apparatus is readily apparent in ependymal and tracheal cilia of wild-type mice (Fig. 2, e, f, i, and j). The relative lengths of the four major CP projections (C1a, C1b, C2a, and C2b) differ in *C. reinhardtii* and *Mus musculus* but conserved details of CP structure allowed us to apply the nomenclature established for the CP projections of *C. reinhardtii* (Mitchell and Sale, 1999) to the cilia of mice, as shown in Fig. 2. Markers of CP asymmetry present in mice and *C. reinhardtii* include two rod-shaped projections (C1c and C1d) on the C1 microtubule, a knob-shaped projection (C2c) associated with the C2 microtubule (Fig. 2, e and i), and a diagonal link that connects the C1b projection with the C2 microtubule (Fig. 2, e and j, arrowhead).

Cross sections through ependymal cilia from *hy3/hy3* animals revealed that the central apparatus lacked projection C2b (*n* = 28 from two mice on P6 and 7; Fig. 2, g and h). Additionally, projection C1b was often displaced or altered in shape and projection C2c was frequently (~55%) diminished or absent. Cilia in the trachea of *hydin* mutants similarly lacked the C2b projection and had altered C1b and C2c projections (*n* = 13 from two mice; Fig. 2, k and l). The general ultrastructure of the CP and the defects observed in mutant animals are revealed clearly in image averages (Fig. 2, f, h, j, and l). In summary, Hydin deficiency in mice results in the loss of CP projection C2b with accompanying changes to the two adjacent projections.

Ciliary bending is impaired in *hydin* mutants

To determine how these CP defects affected the motility of cilia in *hydin* mutant mice, we observed and recorded side, front, and top views of ependymal cilia (Fig. S2, available at http://www.jcb.org/cgi/content/full/jcb.200710162/DC1). The ependymal cilia of wild-type animals (*n* = 10) exhibited a highly asymmetrical ciliary beat (Fig. 3 a and Video 1). The beat began with the formation of a large bend at the base of the cilium that swept the cilium forward in a effective stroke (Fig. 3 c) followed by propagation of the bend during the recovery stroke to return the cilium to its starting position (Fig. 3 d). In contrast, the cilia of *hy3/hy3* (*n* = 6) and *OVE459* (*n* = 3) animals appeared to vibrate stiffly without forming distinct effective or recovery strokes (Fig. 3 b and Video 2). Instead, they formed a bend that was
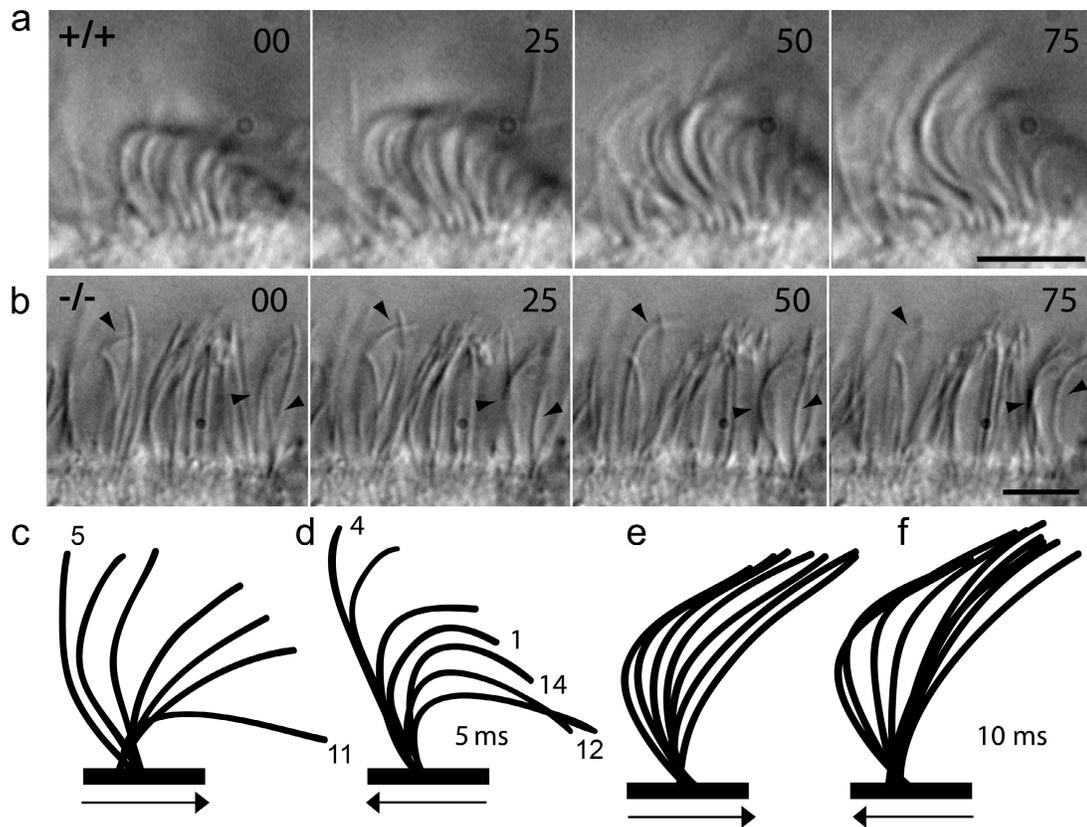
Figure 3. **Impaired ciliary bending in *hydin* mutants.** Sequential still images of ependymal cilia from the wild type (+/+; a) and a *hy3/hy3* mutant (−/−; b). The time is indicated in milliseconds. In b, three moving cilia are tracked with arrowheads. Bars, 5 μm. (c–f) Ciliary waveform in the wild type (c and d) and Hydin mutants (e and f). Line tracings of the effective stroke (c and e) and the recovery stroke (d and f) are shown. In c and d, the frame numbers are indicated. Ciliary positions are shown every 5 or 10 ms for the wild type and mutant, respectively. The line tracings are from different videos than those shown in panels a and b; e and f are from an *OVE459* animal. Arrows indicate the direction of movement of the cilia.

smaller than that of the wild type and spread over the proximal 1/2–2/3 of the cilium (Fig. 3 f); the bend then appeared to relax with little propagation, returning the cilium to an unbent position (Fig. 3 e and see Fig. 4 h). Stiff vibrating cilia were similarly observed in trachea of mutant animals, whereas the characteristic ciliary bending pattern was observed in wild-type trachea (Videos 3 and 4). Therefore, Hydin deficiency severely impairs the beat pattern of ependymal and tracheal cilia.

Cilia in *hydin* mutants have a planar waveform but tend to stall

Normal 9 + 2 epithelia cilia show a relatively planar back-and-forth motion, whereas the 9 + 0 airway cilia from patients lacking the CP perform an unusual whirling type of movement (Chilvers et al., 2003). This suggests that the mammalian CP is necessary for maintaining a planar waveform. The analysis of top views of ependymal cilia from wild-type and mutant animals revealed that both had a near planar beat envelope (Fig. 4, a and b). Thus, the absence of the C2b projection in Hydin-deficient mice does not prevent the cilia from beating with a planar waveform.

Frame-by-frame analysis revealed that cilia from *hy3/hy3* but not wild-type mice frequently stalled at the transition points between the effective and recovery strokes (Fig. 4, a, b, and h). Fig. 4 (c–g) shows line scans within the plane of the beat of mutant and wild-type cilia; the stalling is visible as regular plateaus at

the peaks and valleys of the line scans for the mutant cilia. Most wild-type cilia moved almost continuously through the transition between strokes (43% did not stop, 39% were in a similar position in two consecutive frames, and ~19% paused for longer periods averaging 17 ms; $n = 73$ from five animals). In contrast, 79% of Hydin-deficient cilia showed prolonged pauses (mean of 30.1 ± 21.8 ms) and only 5% of the cilia did not stall ($n = 64$ from four animals). Therefore, the Hydin deficiency delayed the switch between the forward and backward motion of the cilia.

Cilia in *hydin* mutants beat at a lower frequency

To determine the ciliary beat frequency (CBF) of wild-type and *hydin* mutant cilia, line scans (kymograms) were obtained from videos showing cilia in top or side views (Fig. 5, a–d). The changes in grayscale over time in these kymograms were plotted (Fig. 5, e and f) and the CBF was calculated (Fig. 5 g). At ambient temperature, ependymal cilia of wild-type animals had a mean CBF of 10.7 ± 3.7 Hz ($n = 16$ based on samples from four wild-type plus one heterozygous animal) compared with 6.8 ± 2.8 Hz for mutant animals ($n = 18$ based on samples from four *hy3/hy3* animals); maximum CBF values were 18 and 12 Hz for wild-type and mutant animals, respectively. Similarly, the CBF of tracheal cilia was reduced in mutants (10.4 ± 1.2 Hz) in comparison with the wild type (15.7 ± 3.1 Hz) based on measurements on five
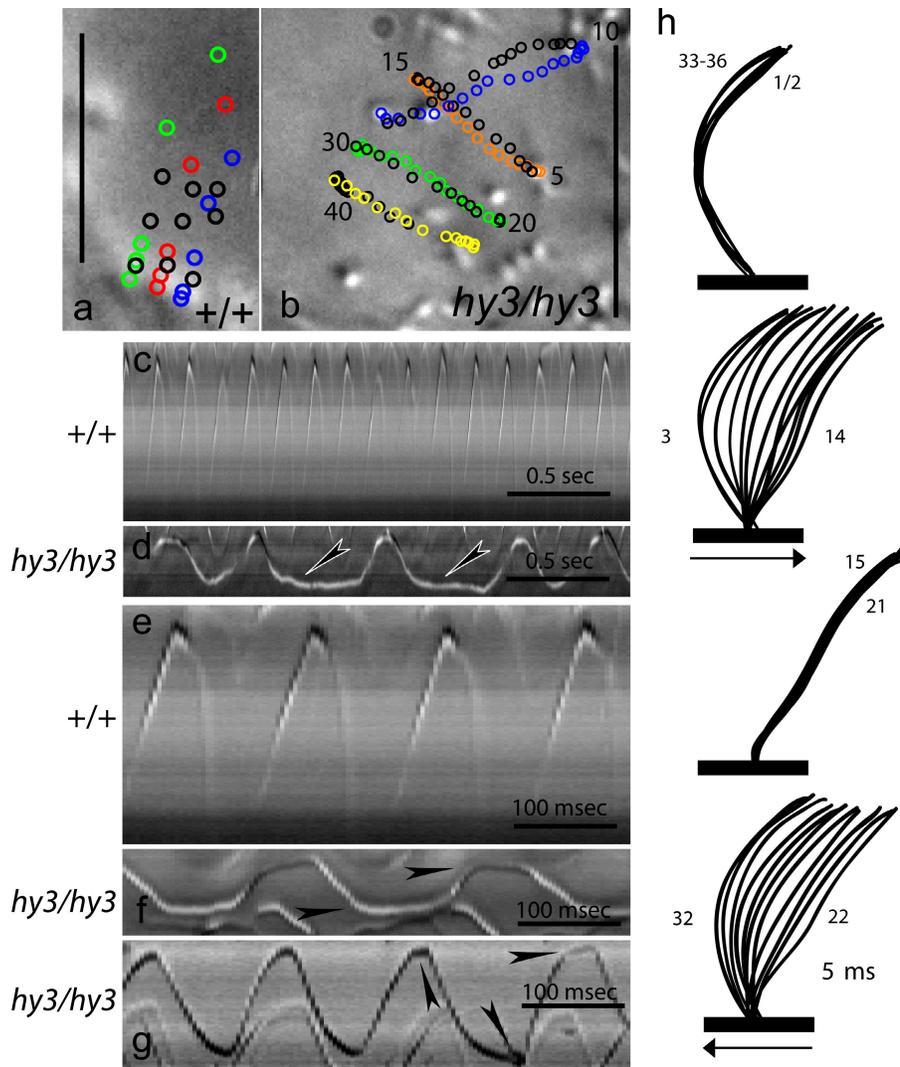
Figure 4. **Stalling of cilia in *hydin* mutants.** (a and b) Top views of ependymal cilia were analyzed frame-by-frame and the positions of selected cilia were marked by circles in different colors. The time between frames was 5 ms. The color of the circles was changed to black when a cilium changed direction. Wild-type cilia (a) smoothly transitioned from forward to backward movement, whereas mutant cilia (b) frequently stalled at the turnaround points as indicated by the accumulation of marks. The duration (in milliseconds) of stalling is indicated. Bars, 5 μm. (c–g) Line scans through the plane of beat from individual wild-type (c and e) and mutant (d, f, and g) ependymal cilia observed in the top view. Stalling of mutant cilia frequently resulted in plateaus at the peaks and valleys of the line scans (arrowheads). (h) Frame-by-frame line tracings of a complete beat cycle of an ependymal cilium from a *hy3/hy3* animal. 36 consecutive frames are shown and some are numbered. The time between lines corresponds to 5 ms and the arrows indicate the direction of movement of the cilium. Note the extended rest times at the turnaround points (first and third sets of tracings).

and six samples, respectively, from one *OVE459* mutant animal and one wild-type littermate (Fig. 5 h).

Wild-type cilia also move with higher velocity during their effective and recovery strokes than do mutant cilia (Fig. 3, compare c and d with e and f; note that the tracings were made every 5 ms in the former and every 10 ms in the latter). Stalling and the reduced velocity during the strokes accounts for the reduced CBF of the mutant cilia.

Hydin deficiency reduces coordination between cilia

We further noted that the polarity of beat of the ependymal cilia in *hydin* mutants was defective. In wild-type ependymal cells, the plane of beat is similar for most of the cilia (Fig. 6 a). Accordingly, lines used to visualize these planes are mostly parallel (standard deviation of 16.8°, $n = 54$ cilia; Fig. 6 b). In contrast, the beat planes of cilia from mutants are much less well-ordered (standard deviation of 36°, $n = 42$ cilia; Fig. 6, c and d). This impaired their ability to move in an organized manner. Wild-type cilia exhibited metachronal beating, which was revealed as regular diagonal lines on kymograms (Fig. 6, e and f). In contrast, Hydin-deficient cilia did not display metachrony; line scans of

cilia from mutant ependymal epithelia consisted mostly of curves representing individual cilia (Fig. 6, g and h). Thus, Hydin deficiency reduces the coordination between ependymal cilia.

The basal foot is a cone-shaped structure attached to the basal body and it is thought that the ciliary beat plane is related to the position of the basal foot. In wild-type tracheal cells, basal feet were oriented almost perpendicular to the plane through the two central microtubules on the side of the C1b and C2b projections (Fig. S3, a–d, available at http://www.jcb.org/cgi/content/full/jcb.200710162/DC1; $n = 4$ tracheal cells from two mice). The angle between basal feet in the wild type varied by just 16.9 ± 5.1° ($n = 21$ basal feet from two ependymal cells; Fig. 6 i). This angle was much more variable in ependymal cells from mutant animals (58.6 ± 18°, 81 basal feet in 11 ependymal cells; Fig. 6 f), which indicates that the lack of Hydin causes a reduced alignment of neighboring cilia. Even though basal feet in mutants are more variable in their orientation, they generally point in the direction of the C1b projection and the now-missing C2b projection, which suggests that the CP retains its correct fixed position relative to the outer doublets even in mutant animals ($n = 5$ ependymal cells; Fig. S3 e). Basal feet also lack alignment in PCD patients missing dynein arms (Afzelius, 1980) and in *Xenopus laevis*
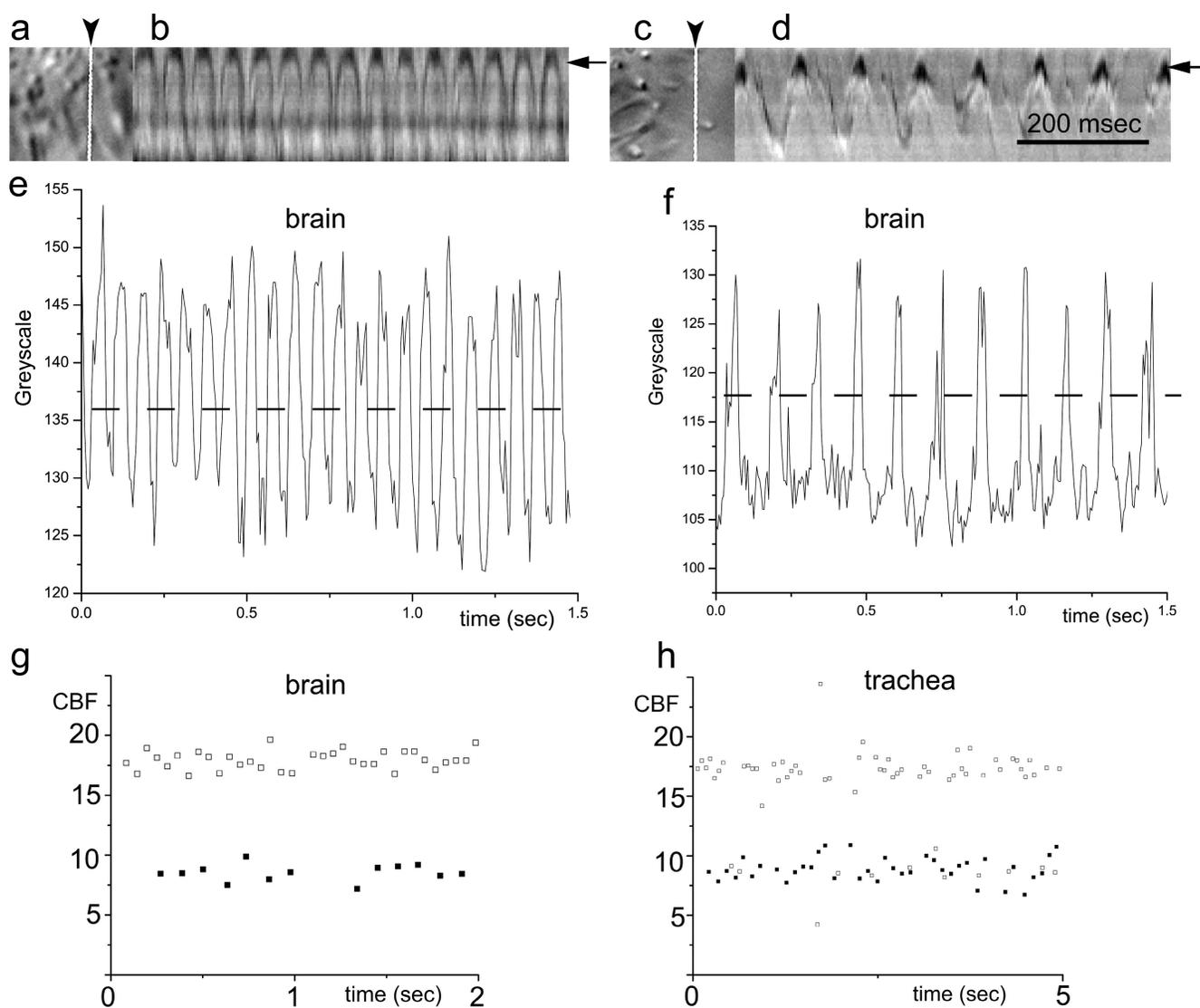
Figure 5. **CBF is reduced in *hydin* mutants.** Images from videos (a and c), line scans (b and d), and corresponding plots (e and f) of ependymal cilia from wild-type (a, b, and e) and mutant animals (c, d, and f). The position of the line used for preparing the line scan is indicated in panels a and c (arrowhead and white line); the part of the line scan used for preparing the plots is indicated in b and d (arrow). (g) CBF for wild-type (open squares) and mutant (closed squares) animals based on the plots shown in e and f. (h) CBF of tracheal cilia in samples from a hydrocephalic *OVE459* mutant (closed squares) and a wild-type littermate (open squares).

embryos with defective cilia (Mitchell et al., 2007), which indicates that cilia-generated fluid flow is required for the alignment of cilia. Therefore, the effect of Hydin deficiency on ciliary orientation is likely to be caused indirectly by the impairment of fluid flow (see the following section).

Hydin deficiency impairs cilia-generated flow
To determine how the mutant cilia affected fluid flow, polystyrene beads (0.5 μm in diameter) were added to brain slices of two mutant *OVE459* animals and two wild-type littermates. Particles moved fast and directionally along the ependyma of wild-type mice (Fig. 7 a and Video 5, available at http://www.jcb.org/cgi/content/full/jcb.200710162/DC1). The velocity of individual particles varied with the distance from the cilia; near the epidermis, velocities of 80–120 μm/s were observed. In contrast, the particles vibrated in place or moved only slowly over the ependyma of

mutant mice (∼10 μm/s; Fig. 7 b and Video 6). Similar results were observed for *hy3/hy3* animals and their wild-type littermates (unpublished data). Rapid directional movement also was observed for polystyrene beads added to slices of trachea from wild-type animals (Fig. 7 c), whereas a directional movement of particles was not observed with samples from mutant trachea (Fig. 7 d). In conclusion, the cilia-generated fluid flow in the ventricles and trachea is greatly impaired by the Hydin deficiency.

Discussion

Ablation of *Hydin* results in loss of the same CP projection in both *C. reinhardtii* and mice
Ultrastructural analysis of cilia from *hydin* mutant mice revealed that the dynein arms, radial spokes, and CP were present
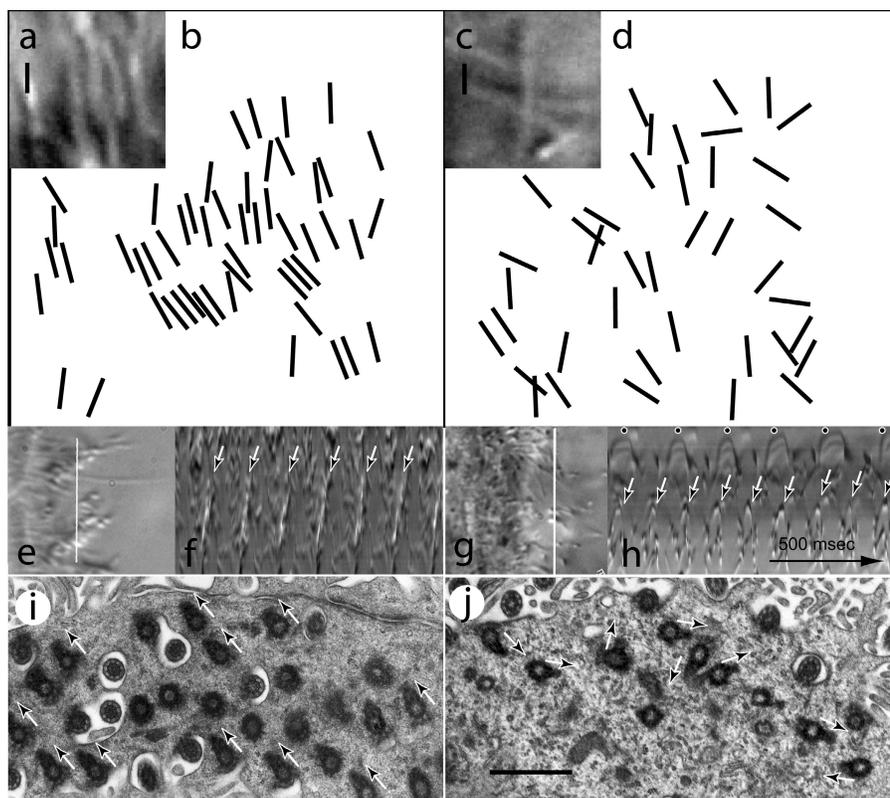
Figure 6. **Reduced ciliary coordination in *hydin* mutants.** Images and image analysis from the wild-type (a, b, e, f, and i) and mutant brain (c, d, g, h, and j). (a and c) Average of eight frames of ependymal cilia in top view; moving cilia appear as lines. (b and d) The plane of ciliary beating was marked by lines using three images, each representing an average of eight frames and showing cilia in top view. (e–h) Images (e and g) showing the lines used to generate scans and the corresponding line scans (kymograms; f and h). (f) The diagonal lines marked by arrows result from the coordinated sequential movement of wild-type cilia. (h) The line scans for the mutant break up into tracks of individual cilia, revealing their different CBFs (arrows and dots). The horizontal parts of the scan marked by dots indicate stalling of the cilium. (i and j) Orientation of the basal feet in the ependymal epithelium from wild-type (i) and mutant (j) animals. Bars, 1 µm.

but that one of the projections was missing from the central apparatus. Similarly, hydin knockdown in *C. reinhardtii* resulted in the loss of a CP projection (Lechtreck and Witman, 2007). The ultrastructure of the CP, like that of most of the rest of the axoneme, is well conserved; negatively stained whole mounts from rat sperm and *C. reinhardtii* flagella have shown that one of the microtubules (C2) has projections that repeat at 16-nm intervals, whereas the other (C1) has projections with both 16- and 32-nm repeats (Olson and Linck, 1977; Mitchell, 2003, 2004). The asymmetry of the CP is also evident in cross sections through the cilia of mice and *C. reinhardtii*, and we were able to apply the nomenclature used to label individual projections in *C. reinhardtii* to the CP of mice. The results indicate that the CPs of Hydin-deficient cilia/flagella from mice and *C. reinhardtii* have an identical ultrastructural defect, the absence of projection C2b.

Mammalian Hydin is required for proper control of the dynein arms

The lack of Hydin in mice restricted the ability of the cilia to bend. Wild-type cilia generate a strong bend near the base of the cilium during the effective stroke and propagate this bend to the tip of the cilium during the recovery stroke. Cilia of *hydin* mutants lack the ability to focus the bending to a restricted part of the cilium and then propagate it along its length; instead they alternate between an almost uniformly curved shape and an almost straight shape. This stiff forward-backward movement resembles the motion of cilia with defects in the inner dynein arms or radial spokes in human PCD patients (Chilvers et al., 2003), which suggests that the absence of Hydin specifically affects the CP–radial spoke–inner dynein arm control pathway. This movement

is in contrast to the circular beat pattern observed in cilia from PCD patients lacking the complete CP or the almost complete paralysis observed for cilia from PCD patients lacking the outer arms (Chilvers et al., 2003; Stannard et al., 2004; Carlen and Stenram, 2005). The fact that the Hydin-deficient mice cilia still beat in a plane shows that Hydin and the C2b projection of the CP are not required to maintain a planar beat. We further observed that the mutant cilia move with a reduced velocity, which suggests a role for the CP in controlling the speed of dynein-driven interdoublet sliding. This notion is supported by observations on the *C. reinhardtii* CP complex 1 mutant (*cpc1*), which lacks the C1b projection and displays normal flagellar bending patterns but has a reduced CBF (Mitchell and Sale, 1999).

Mice cilia lacking Hydin frequently stall, usually at the positions where the direction of beat changes. This defect closely resembles aspects of the phenotype caused by hydin knockdown in *C. reinhardtii* (Lechtreck and Witman, 2007). The flagella of *C. reinhardtii* hydin RNAi cells were arrested randomly at the beginning or end of the effective and recovery strokes, and flagella with residual motility often paused in these positions. At these points of reversal of beat direction, the activity of the dynein arms needs to be switched from one side of the axoneme to the other (Satir and Matsuoka, 1989; Nakano et al., 2003; Wargo et al., 2004). Because the hydin-deficient *C. reinhardtii* flagella were arrested at these switch points, it was hypothesized that hydin is involved in turning the arms on or off in opposite halves of the axoneme. The stalling of the Hydin-deficient mouse cilia suggests that mammalian Hydin is similarly involved in regulating the dynein arms during the transitions between effective and recovery strokes.
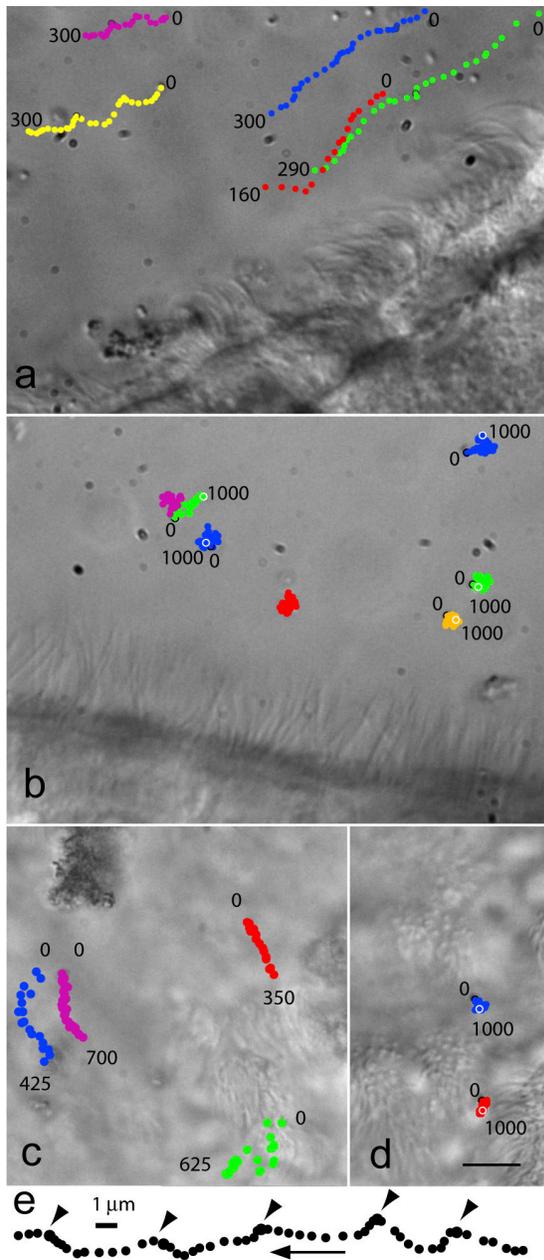
Figure 7. **Cilia of Hydin-deficient mice fail to produce a flow.** Analysis of cilia-generated fluid flow in the third ventricle (a and b; side view) and in trachea (c and d; top view). The positions of polystyrene particles on selected video frames were marked with colored dots; the distance between neighboring dots is 10 (a), 25 (b and c), or 50 ms (d). The time represented by each trace is noted for some particles. Rapid directional movement was observed with wild-type samples (a and c), whereas flow was absent or severely reduced in the mutant (b and d). Bar, 5 μm. (e) Detailed track of a particle from flow analysis in wild-type brain sections; the distance between dots is 5 ms. The arrowheads mark the periodic changes in velocity and direction of the particle. The arrow indicates direction of movement.

The apparent conservation of both the structural and functional roles of Hydin in *C. reinhardtii* and mammals is remarkable given major differences in the operation of the axonemal machinery. In *C. reinhardtii*, the CP is twisted and rotates within the axonemal shaft (Mitchell and Nakatsugawa, 2004). Therefore, the CP continuously changes its position relative to the outer doublets, and an individual projection could influence the

activity of dyneins on different doublets. In mammals, the CP is in a fixed position and does not rotate, so that a given projection always faces the same group of doublets. Because the basal foot points in the direction of the effective stroke (Gibbons, 1961; Mitchell et al., 2007), the C2b projection faces a subset of those doublets that would be active during the effective stroke (Fig. S3, b and c). It is possible that in the Hydin-deficient mice cilia, these arms fail to be activated, leading to an effective stroke with an attenuated bend. Moreover, if the normal sequential activation of the arms were interrupted at this point, the arms in the opposite half of the axoneme might fail to be activated so that the cilium relaxes and returns passively to its unbent position. In this case, the cilium would appear to bend in only one direction, as observed for the Hydin-deficient mice cilia. Consistent with such a hypothesis, it should be noted that because both bending and beat frequency are much reduced in the Hydin-deficient mice cilia compared to wild-type cilia, the total amount of dynein-driven interdoublet sliding must be greatly reduced in the mutant axonemes.

Impaired ciliary motility causes hydrocephalus in *hydin* mutants

The abnormal motility of the mutant cilia greatly reduced or eliminated the flow generated by the ependymal cilia. This lack of flow is likely to be the underlying cause of the development of hydrocephalus in these mutants. Impaired ciliary or flagellar motility also has been reported in mice lacking the axonemal dynein heavy chain Mdnah5 or the CP protein sperm-associated antigen 6 (Spag6; Ibanez-Tallon et al., 2002; Sapiro et al., 2002; Zhang et al., 2007). *Mdnah5* mutants have severely abnormal motility of the ependymal cilia and reduced ependymal flow (Ibanez-Tallon et al., 2004). Mice deficient in Spag6 display significantly reduced sperm motility (Sapiro et al., 2002). Both mutations produce hydrocephalus. This, collectively with our findings, indicates that impaired ciliary motility alone is sufficient to cause hydrocephalus in mice. In the *mdnah5* homozygous mice, stenosis of the cerebral aqueduct between the third and fourth ventricles was observed on P6; this resulted in triventricular hydrocephalus with massive enlargement of the third ventricle, whereas the fourth ventricle did not enlarge (Ibanez-Tallon et al., 2004). Therefore, it was proposed that ciliary motility is required to keep the narrow cerebral aqueduct open.

Hydrocephalus also occurs in *tg737^{orpk}* mutant mice (Banizs et al., 2005). These mice are homozygous for a hypomorphic allele of IFT88/polaris, a component of the intraflagellar transport machinery required for the assembly of motile and immotile cilia (Pazour et al., 2000). As a consequence, the mice develop cilia-related defects, including polycystic kidney disease and retinal degeneration, and the ependymal cilia are malformed and fail to generate ependymal flow. The cerebral aqueduct becomes blocked by P6, but the first signs of disease are evident before blockage is apparent. Therefore, it has been suggested that defects in the primary cilia on the choroid plexus of *tg737^{orpk}* mutant mice result in an overproduction of cerebrospinal fluid leading to hydrocephalus (Banizs et al., 2005, 2007). This precise scenario is unlikely for *hydin* and *spag6* mutants because the defective gene products are located in the CP, which is absent

in primary cilia. Furthermore, these mutants lack the pleiotropic disorders characteristic of mutants having defective primary cilia (Badano et al., 2006). However, one cannot rule out the possibility that defects in the motile cilia of the choroid plexus or the ependyma cause cerebrospinal fluid overproduction by impairing the proper distribution of factors required to control its production.

Loss of Hydin does not cause situs inversus

The nodal cilia of mice embryos undergo an unusual whirling movement that generates a leftward flow of extraembryonic fluid that is required for the establishment of left–right asymmetry; an inability to assemble these cilia or impairment of their motility results in the randomization of left–right asymmetry (Nonaka et al., 1998; Ibanez-Tallon et al., 2002). Although nodal cilia have generally been thought to have a 9 + 0 axoneme lacking a CP, central microtubules recently were observed in some cilia of the mouse node and in up to 62% of the cilia in certain regions of the notochordal plate (equivalent to the mouse node) in rabbits, which raises questions about the function of the CP in these cilia (Feistel and Blum, 2006; Caspary et al., 2007). Our observation that *hydin* mutant mice lack situs abnormalities indicates that Hydin, at least, has no important role in generating the whirling motility of nodal cilia. Similarly, mutation of the CP protein Spag6 in mice does not cause situs abnormalities (Sapiro et al., 2002). Neither have situs abnormalities been observed in PCD patients with CP defects (Sturgess et al., 1979; Tamalet et al., 2001; Chilvers et al., 2003; Stannard et al., 2004; Carlen and Stenram, 2005). These observations strongly suggest that the CP itself is not required for the whirling motion characteristic of nodal cilia (Okada et al., 2005) and, consequently, CP defects do not result in situs abnormalities. Consistent with this, all posterior notochordal cilia in the rabbit exhibit a whirling movement (Okada et al., 2005; Feistel and Blum, 2006) even though some of these cilia have central microtubules and others do not.

HYDIN, CP defects, and human disease

In the *hydin* mutant mice, the motility of the tracheal cilia also was severely impaired. Therefore, we would expect that humans with defects in *HYDIN* would have ciliary dyskinesia and develop PCD, although without accompanying situs inversus (see previous section). Definitive diagnosis of PCD in patients without situs inversus traditionally requires the demonstration of loss of an axonemal structure (in airway cilia or sperm flagella) by EM and/or the demonstration of defective ciliary movement on airway cells obtained by nasal brushing or biopsy (Meeks and Bush, 2000; van's Gravesande and Omran, 2005). Based on our results, defects in human *HYDIN* would cause a subtle ultrastructural defect that might easily escape EM analysis. In fact, in at least 3% of PCD patients, no ultrastructural defect is observed. In such patients, we suggest that particular care should be given to examination of the CP. Similarly, defects in human *HYDIN* would be expected to cause a relatively small reduction in beat frequency that might not be noticed by methods that examine CBF but not waveform or the ability to generate fluid flow. Therefore, if nearly normal CBF is found in suspected PCD

patients, the waveform and coordination of the cilia should be examined for abnormalities, ideally by high-speed video microscopy (Chilvers et al., 2003; Noone et al., 2004).

Are defects in *HYDIN* likely to cause hydrocephalus in humans? As noted in the Introduction, a mutation causing hydrocephalus has been mapped to within 1.2 Mb of the *HYDIN* locus at 16q22.2-q22.3 (Callen et al., 1990). Although not all patients with defects in motile cilia develop hydrocephalus, there are numerous cases where an association between PCD and hydrocephalus has been reported (De Santi et al., 1990; al-Shroof et al., 2001; Kosaki et al., 2004), and the incidence of hydrocephalus caused by aqueduct stenosis in PCD patients is estimated to be $\sim$83$\times$ higher than in the general population (Ibanez-Tallon et al., 2004). It is likely that morphological differences such as the diameter of the cerebral aqueduct in the developing brain are responsible for the different effects of dysmotile cilia on humans, where immotile cilia most commonly cause PCD, and mice, where defects in motile cilia almost always cause hydrocephalus. In any case, we predict that dysmotile cilia caused by defects in *HYDIN* will increase the risk of hydrocephalus in humans.

Materials and methods

Mice
The two mutant hydin alleles, *hy3* and *OVE459*, were maintained heterozygously in an FVB/N background (Robinson et al., 2002). All animal procedures were performed in accordance with the National Research Council's Guide for the Care and Use of Laboratory Animals. PCR-based genotyping to identify *hy3/hy3* homozygotes and to test for the presence of the inserted transgene in *OVE459* animals was performed as described previously (Robinson et al., 2002; Davy and Robinson, 2003) with modification for real-time PCR (wild-type and *hy3* allele: 7 min at 95°C, 38× [40 s at 94°C, 40 s at 55.5°C, and 50 s at 72°C], and 10 min at 72°C; *OVE459* transgene: 7 min at 95°C, 35× [40 s at 94°C, 50 s at 58°C, and 45 s at 72°C], and 10 min at 72°C).

Video microscopy of ependymal and tracheal cilia
Animals were killed by intraperitoneal injection of pentobarbital sodium. Brains were removed, washed in HBSS (Invitrogen) supplemented with 25 mM Hepes (sHBSS, pH 7.4), trimmed for sagital or coronal sectioning of the third and lateral ventricles, and sectioned into 130-µm slices using a vibratome (OTS-4000; Electron Microscopy Sciences). Sections in sHBSS were observed with differential interference contrast microscopy using an inverted microscope (IX71; Olympus) equipped with a 60× water immersion objective (numerical aperture 1.20) and a zoom adaptor (Nikon). Images (640 pixels × 480 lines) of ciliary activity were recorded at 200 frames per second with a high-speed, progressive scan charge-coupled device camera (TM-6740; Pulnix) and image acquisition software (Video Savant; IO Industries) as described previously (Zhang and Sanderson, 2003; Delmotte and Sanderson, 2006). Samples were analyzed at room temperature typically within 25–60 min after euthanasia; importantly, cilia continued to beat rapidly for 24 h in slices incubated in Dulbecco's Modified Eagle's Medium supplemented with 10% FBS, penicillin, and streptomycin at 37°C in 10% CO_2. The CBF of ependymal cilia was calculated as described in Results. To visualize cilia-generated fluid flow, sections with an exposed third ventricle were placed into chambers and polystyrene beads (0.5 µm in diameter; Sigma-Aldrich) were added.

For study of airway cilia, trachea were removed, cleaned under a dissecting microscope, cut into rings or strips to record side and top views, respectively, and observed as described in the preceding paragraph. The CBF of tracheal cilia was measured as described previously (Delmotte and Sanderson, 2006).

For still images and slow-motion videos, individual frames were cropped and adjusted for brightness and contrast in Photoshop (Adobe). Figures were assembled using Illustrator (Adobe). Line scans (kymograms) were prepared by extracting a row of pixels from each image of a series and placing them sequentially in time to create a single image using Scion Image

(Scion Corporation). Videos were made using QuickTime 7.2 (Apple). To analyze the movement of individual cilia, frames were copied from QuickTime movies into Illustrator, and cilia were traced using the paintbrush tool. When the target cilium was not entirely visible, missing parts were filled in based on observations made on other cilia.

Ultrastructural analysis of cilia
Brain slices and trachea ring sections were made as described in the previous section or thicker slices were made by hand and fixed for 2 h with 2% glutaraldehyde and 2.5% formaldehyde in 75–100 mM cacodylate buffer. After several washes in buffer, the tissues were treated with 1% OsO_4 for 1 h. For TEM, fixed specimens were washed twice with buffer and twice with water and incubated overnight in aqueous 1% uranyl acetate at 4°C. After several washes in water, the slices were dehydrated, embedded, and sectioned using standard procedures. Brain slices were flat embedded and then mounted onto epon blocks to ensure proper orientation of the cilia. Thin sections were analyzed using CM10 and CM12 electron microscopes (Philips). For SEM, samples were washed and dehydrated after OsO_4 fixation (see TEM fixation protocol), critically point dried, coated with a 4-nm-thick layer of iridium, and examined using a field emission SEM (Quanta 200F; FEI). Averaged images were prepared with Photoshop.

Immunofluorescence microscopy
For immunofluorescence microscopy, freshly prepared trachea from a 6-d-old mutant and a 5-d-old wild-type animal were brushed with a wooden stick, washed into HBSS supplemented with 25 mM Hepes, pH 7.4, centrifuged onto poly-L-lysine–coated coverslips, fixed with methanol at −20°C for 8 min, dried, and then blocked with PBS containing 0.05% Tween 20, 3% fish gelatin, and 1% BSA for 30 min. Anti-acetylated tubulin (1:800; Sigma-Aldrich) was applied overnight at 4°C and goat anti–mouse F(ab)$_2$ of IgG Alexa Fluor 488 (1:400; Invitrogen) was applied for 90 min. Images were acquired using Axiovision software and a camera (AxioCam MRm) on a microscope (Axioskop 2 Plus) equipped with a 100× 1.4 numerical aperture oil differential interference contrast Plan Apochromat objective (all from Carl Zeiss, Inc.) and epifluorescence. Image brightness and contrast were adjusted using Photoshop 5.0. Figures for publication were assembled using Illustrator 8.0. Capture times and adjustments were similar for images mounted together.

Online supplemental material
Fig. S1 shows SEM images of brain and trachea from wild-type and *hy3/hy3* animals demonstrating that the assembly of cilia is not affected by the loss of Hydin. Epithelial cells from trachea were also stained with anti-acetylated tubulin for immunofluorescence to show the presence of full-length cilia. Fig. S2 shows two video frames each of side, front, and top views of wild-type ependymal cilia. Fig. S3 shows TEM images of a wild-type epithelial cell from the trachea in overview and detail revealing that the CP projection C2b points in the same direction as the basal foot, a marker pointing in the direction of the power stroke. Videos 1 and 2 show the motility of ependymal cilia from wild-type and *hydin* mutant animals, respectively. Videos 3 and 4 show the motility of tracheal cilia from wild-type and *hydin* mutant animals, respectively. Videos 5 and 6 show the flow generated by wild-type and mutant ependymal cilia. Online supplemental material is available at http://www.jcb.org/cgi/content/full/jcb.200710162/DC1.

References

Afzelius, B.A. 1980. Genetic disorders of cilia. *In* International Cell Biology 1980-81, H.G. Schweiger, editor. Springer-Verlag, Berlin. 440-447.

Afzelius, B.A. 1999. Asymmetry of cilia and of mice and men. *Int. J. Dev. Biol.* 43:283–286.

al-Shroof, M., A.M. Karnik, A.A. Karnik, J. Longshore, N.A. Sliman, and F.A. Khan. 2001. Ciliary dyskinesia associated with hydrocephalus and mental retardation in a Jordanian family. *Mayo Clin. Proc.* 76:1219–1224.

Badano, J.L., N. Mitsuma, P.L. Beales, and N. Katsanis. 2006. The ciliopathies: an emerging class of human genetic disorders. *Annu. Rev. Genomics Hum. Genet.* 7:125–148.

Banizs, B., M.M. Pike, C.L. Millican, W.B. Ferguson, P. Komlosi, J. Sheetz, P.D. Bell, E.M. Schwiebert, and B.K. Yoder. 2005. Dysfunctional cilia lead to altered ependyma and choroid plexus function, and result in the formation of hydrocephalus. *Development.* 132:5329–5339.

Banizs, B., P. Komlosi, M.O. Bevensee, E.M. Schwiebert, P.D. Bell, and B.K. Yoder. 2007. Altered pH(i) regulation and Na(+)/HCO3(−) transporter activity in choroid plexus of cilia-defective Tg737(orpk) mutant mouse. *Am. J. Physiol. Cell Physiol.* 292:C1409–C1416.

Broadhead, R., H.R. Dawe, H. Farr, S. Griffiths, S.R. Hart, N. Portman, M.K. Shaw, M.L. Ginger, S.J. Gaskell, P.G. McKean, and K. Gull. 2006. Flagellar motility is required for the viability of the bloodstream trypanosome. *Nature.* 440:224–227.

Callen, D.F., E.G. Baker, and S.A. Lane. 1990. Re-evaluation of GM2346 from a del(16)(q22) to t(4;16)(q35;q22.1). *Clin. Genet.* 38:466–468.

Carlen, B., and U. Stenram. 2005. Primary ciliary dyskinesia: a review. *Ultrastruct. Pathol.* 29:217–220.

Caspary, T., C.E. Larkins, and K.V. Anderson. 2007. The graded response to Sonic Hedgehog depends on cilia architecture. *Dev. Cell.* 12:767–778.

Chilvers, M.A., A. Rutman, and C. O'Callaghan. 2003. Ciliary beat pattern is associated with specific ultrastructural defects in primary ciliary dyskinesia. *J. Allergy Clin. Immunol.* 112:518–524.

Daniel, G.B., D.F. Edwards, R.C. Harvey, and G.W. Kabalka. 1995. Communicating hydrocephalus in dogs with congenital ciliary dysfunction. *Dev. Neurosci.* 17:230–235.

Davy, B.E., and M.L. Robinson. 2003. Congenital hydrocephalus in hy3 mice is caused by a frameshift mutation in Hydin, a large novel gene. *Hum. Mol. Genet.* 12:1163–1170.

Dawe, H.R., M.K. Shaw, H. Farr, and K. Gull. 2007. The hydrocephalus inducing gene product, Hydin, positions axonemal central pair microtubules. *BMC Biol.* 5:33.

De Santi, M.M., A. Magni, E.A. Valletta, C. Gardi, and G. Lungarella. 1990. Hydrocephalus, bronchiectasis, and ciliary aplasia. *Arch. Dis. Child.* 65:543–544.

Delmotte, P., and M.J. Sanderson. 2006. Ciliary beat frequency is maintained at a maximal rate in the small airways of mouse lung slices. *Am. J. Respir. Cell Mol. Biol.* 35:110–117.

Doggett, N.A., G. Xie, L.J. Meincke, R.D. Sutherland, M.O. Mundt, N.S. Berbari, B.E. Davy, M.L. Robinson, M.K. Rudd, J.L. Weber, et al. 2006. A 360-kb interchromosomal duplication of the human HYDIN locus. *Genomics.* 88:762–771.

Dutcher, S.K., B. Huang, and D.J. Luck. 1984. Genetic dissection of the central pair microtubules of the flagella of *Chlamydomonas reinhardtii. J. Cell Biol.* 98:229–236.

Feistel, K., and M. Blum. 2006. Three types of cilia including a novel 9+4 axoneme on the notochordal plate of the rabbit embryo. *Dev. Dyn.* 235:3348–3358.

Fliegauf, M., T. Benzing, and H. Omran. 2007. When cilia go bad: cilia defects and ciliopathies. *Nat. Rev. Mol. Cell Biol.* 8:880–893.

Gibbons, I.R. 1961. The relationship between the fine structure and direction of beat in gill cilia of a lamellibranch mollusk. *J. Biophys. Biochem. Cytol.* 11:179–205.

Gruneberg, H. 1943. Two new mutant genes in the house mouse. *J. Genet.* 45:22–28.

Hopkins, J.M. 1970. Subsidiary components of the flagella of *Chlamydomonas reinhardii. J. Cell Sci.* 7:823–839.

Ibanez-Tallon, I., S. Gorokhova, and N. Heintz. 2002. Loss of function of axonemal dynein Mdnah5 causes primary ciliary dyskinesia and hydrocephalus. *Hum. Mol. Genet.* 11:715–721.

Ibanez-Tallon, I., A. Pagenstecher, M. Fliegauf, H. Olbrich, A. Kispert, U.P. Ketelsen, A. North, N. Heintz, and H. Omran. 2004. Dysfunction of axonemal dynein heavy chain Mdnah5 inhibits ependymal flow and reveals a novel mechanism for hydrocephalus formation. *Hum. Mol. Genet.* 13:2133–2141.

Kosaki, K., K. Ikeda, K. Miyakoshi, M. Ueno, R. Kosaki, D. Takahashi, M. Tanaka, C. Torikata, Y. Yoshimura, and T. Takahashi. 2004. Absent inner dynein arms in a fetus with familial hydrocephalus-situs abnormality. *Am. J. Med. Genet. A.* 129:308–311.

Lechtreck, K.F., and G.B. Witman. 2007. *Chlamydomonas reinhardtii* hydin is a central pair protein required for flagellar motility. *J. Cell Biol.* 176:473–482.

Li, J.B., J.M. Gerdes, C.J. Haycraft, Y. Fan, T.M. Teslovich, H. May-Simera, H. Li, O.E. Blacque, L. Li, C.C. Leitch, et al. 2004. Comparative genomics identifies a flagellar and basal body proteome that includes the BBS5 human disease gene. *Cell.* 117:541–552.

Meeks, M., and A. Bush. 2000. Primary ciliary dyskinesia (PCD). *Pediatr. Pulmonol.* 29:307–316.

Mitchell, B., R. Jacobs, J. Li, S. Chien, and C. Kintner. 2007. A positive feedback mechanism governs the polarity and motion of motile cilia. *Nature.* 447:97–101.

Mitchell, D.R. 2003. Orientation of the central pair complex during flagellar bend formation in *Chlamydomonas. Cell Motil. Cytoskeleton.* 56:120–129.

Mitchell, D.R. 2004. Speculations on the evolution of 9+2 organelles and the role of central pair microtubules. *Biol. Cell.* 96:691–696.

Mitchell, D.R., and M. Nakatsugawa. 2004. Bend propagation drives central pair rotation in *Chlamydomonas reinhardtii* flagella. *J. Cell Biol.* 166:709–715.

Mitchell, D.R., and W.S. Sale. 1999. Characterization of a *Chlamydomonas* insertional mutant that disrupts flagellar central pair microtubule-associated structures. *J. Cell Biol.* 144:293–304.

Nakano, I., T. Kobayashi, M. Yoshimura, and C. Shingyoji. 2003. Central-pair-linked regulation of microtubule sliding by calcium in flagellar axonemes. *J. Cell Sci.* 116:1627–1636.

Nonaka, S., Y. Tanaka, Y. Okada, S. Takeda, A. Harada, Y. Kanai, M. Kido, and N. Hirokawa. 1998. Randomization of left-right asymmetry due to loss of nodal cilia generating leftward flow of extraembryonic fluid in mice lacking KIF3B motor protein. *Cell.* 95:829–837.

Noone, P.G., M.W. Leigh, A. Sannuti, S.L. Minnix, J.L. Carson, M. Hazucha, M.A. Zariwala, and M.R. Knowles. 2004. Primary ciliary dyskinesia: diagnostic and phenotypic features. *Am. J. Respir. Crit. Care Med.* 169:459–467.

Okada, Y., S. Takeda, Y. Tanaka, J.C. Belmonte, and N. Hirokawa. 2005. Mechanism of nodal flow: a conserved symmetry breaking event in left-right axis determination. *Cell.* 121:633–644.

Olson, G.E., and R.W. Linck. 1977. Observations of the structural components of flagellar axonemes and central pair microtubules from rat sperm. *J. Ultrastruct. Res.* 61:21–43.

Pazour, G.J., B.L. Dickert, Y. Vucica, E.S. Seeley, J.L. Rosenbaum, G.B. Witman, and D.G. Cole. 2000. *Chlamydomonas* IFT88 and its mouse homologue, polycystic kidney disease gene tg737, are required for assembly of cilia and flagella. *J. Cell Biol.* 151:709–718.

Pazour, G.J., N. Agrin, J. Leszyk, and G.B. Witman. 2005. Proteomic analysis of a eukaryotic cilium. *J. Cell Biol.* 170:103–113.

Raimondi, A.J., S.J. Clark, and D.G. McLone. 1976. Pathogenesis of aqueductal occlusion in congenital murine hydrocephalus. *J. Neurosurg.* 45:66–77.

Robinson, M.L., C.E. Allen, B.E. Davy, W.J. Durfee, F.F. Elder, C.S. Elliott, and W.R. Harrison. 2002. Genetic mapping of an insertional hydrocephalus-inducing mutation allelic to hy3. *Mamm. Genome.* 13:625–632.

Sapiro, R., I. Kostetskii, P. Olds-Clarke, G.L. Gerton, G.L. Radice, and I.J. Strauss. 2002. Male infertility, impaired sperm motility, and hydrocephalus in mice deficient in sperm-associated antigen 6. *Mol. Cell. Biol.* 22:6298–6305.

Satir, P., and T. Matsuoka. 1989. Splitting the ciliary axoneme: implications for a "switch-point" model of dynein arm activity in ciliary motion. *Cell Motil. Cytoskeleton.* 14:345–358.

Smith, E.F. 2002. Regulation of flagellar dynein by the axonemal central apparatus. *Cell Motil. Cytoskeleton.* 52:33–42.

Smith, E.F., and P.A. Lefebvre. 1997. The role of central apparatus components in flagellar motility and microtubule assembly. *Cell Motil. Cytoskeleton.* 38:1–8.

Smith, E.F., and P. Yang. 2004. The radial spokes and central apparatus: mechano-chemical transducers that regulate flagellar motility. *Cell Motil. Cytoskeleton.* 57:8–17.

Stannard, W., A. Rutman, C. Wallis, and C. O'Callaghan. 2004. Central micro-tubular agenesis causing primary ciliary dyskinesia. *Am. J. Respir. Crit. Care Med.* 169:634–637.

Sturgess, J.M., J. Chao, J. Wong, N. Aspin, and J.A. Turner. 1979. Cilia with defective radial spokes: a cause of human respiratory disease. *N. Engl. J. Med.* 300:53–56.

Tamalet, A., A. Clement, F. Roudot-Thoraval, P. Desmarquest, G. Roger, M. Boule, M.C. Millepied, T.A. Baculard, and E. Escudier. 2001. Abnormal central complex is a marker of severity in the presence of partial ciliary defect. *Pediatrics.* 108:E86.

Torikata, C., C. Kijimoto, and M. Koto. 1991. Ultrastructure of respiratory cilia of WIC-Hyd male rats. An animal model for human immotile cilia syndrome. *Am. J. Pathol.* 138:341–347.

van's Gravesande, K.S., and H. Omran. 2005. Primary ciliary dyskinesia: clinical presentation, diagnosis and genetics. *Ann. Med.* 37:439–449.

Wargo, M.J., M.A. McPeek, and E.F. Smith. 2004. Analysis of microtubule sliding patterns in *Chlamydomonas* flagellar axonemes reveals dynein activity on specific doublet microtubules. *J. Cell Sci.* 117:2533–2544.

Witman, G.B., J. Plummer, and G. Sander. 1978. *Chlamydomonas* flagellar mutants lacking radial spokes and central tubules. Structure, composition, and function of specific axonemal components. *J. Cell Biol.* 76:729–747.

Zhang, L., and M.J. Sanderson. 2003. Oscillations in ciliary beat frequency and intracellular calcium concentration in rabbit tracheal epithelial cells induced by ATP. *J. Physiol.* 546:733–749.

Zhang, Z., W. Tang, R. Zhou, X. Shen, Z. Wei, A.M. Patel, J.T. Povlishock, J. Bennett, and J.F. Strauss III. 2007. Accelerated mortality from hydrocephalus and pneumonia in mice with a combined deficiency of SPAG6 and SPAG16L reveals a functional interrelationship between the two central apparatus proteins. *Cell Motil. Cytoskeleton.* 64:360–376.